

Artificial Neural Network Based Load Flow Analysis for Power System Networks

Isaac Samuel, Adebola Soyemi, Ayokunle Awelewa, and Aderibigbe Adekitan.

Abstract—Load flow analysis has become increasingly important as power system expansion now involves unbundling, liberalization, and restructuring networks, putting power system operators in a competitive electricity market. On the other hand, advancements in technology, computing, and software have led to new techniques for carrying out load flow analysis. In this paper, the load flow problem is approached using two techniques: the traditional load flow analysis using the Newton-Raphson method and a non-conventional method using an artificial neural network. This paper presents a load flow solution using the developed artificial neural network on the IEEE 14-bus system and the Nigerian 330kV 28-bus national grid. The results show that load flow analysis can be carried out using the developed artificial neural network with negligible errors between the actual values of voltage magnitudes and voltage phase angles and the neural network output, thus validating the proposed approach. Using the proposed approach, an R-value of 0.9884 and a mean square error of 1.6701×10^{-3} was obtained for the IEEE 14-bus system. For the Nigerian 330kV 28-bus national grid, an R-value of 0.99972 and a mean square error of 3.8624×10^{-3} . MATLAB's neural network toolbox was used to design, develop, and train the artificial neural network used in this paper.

Index Terms—ANN, Load flow analysis, MATLAB, NNG

I. INTRODUCTION

Power system networks (PSNs) have become increasingly complex. Technical, economic, and environmental constraints necessitate the need to optimize the operation of these PSNs; this can be done by carrying out detailed studies that promote the efficient planning and operation of PSNs. Hence, the need for load flow analysis, which can be performed in a steady-state condition. The analysis help determines quantities like line flow, power flow (real and reactive powers), voltage magnitude, and voltage phase angle for specific buses in the PSNs.

Load Flow Analysis (LFA) is a non-linear problem, and as such, it requires the use of iterative methods to get acceptable solutions.

Manuscript received January 21, 2020; revised January 16, 2021. This work was financially supported by Covenant University Center for Research, Innovation and Discovery (CUCRID).

Isaac Samuel is a senior lecturer in the Electrical and Information Engineering Department, Covenant University, Ota, Nigeria. (E-mail: Isaac.samuel@covenantuniversity.edu.ng)

Adebola Soyemi is a master's student in the Electrical and Information Engineering Department, Covenant University, Ota, Nigeria. (E-mail: sadebola@gmail.com)

Ayokunle Awelewa is a fellow in Electrical and Electronics Engineering, Tshwane University of Technology, Pretoria, South Africa. (E-mail Department: ayokunle.awelewa@covenantuniversity.edu.ng)

Aderibigbe Adekitan is a student in the Institute of Electric Power and Control Engineering, Technische Universitat, Ilmenau, Germany. (E-mail: aderibigbe-israel.adekitan@tu-ilmenau.de)

These iterative methods use complex non-linear equations and are time-consuming. These highlighted drawbacks make it necessary to find other techniques to carry out the analysis using non-conventional techniques such as Artificial Intelligence based approaches like fuzzy logic, artificial neural network (ANN), and many others listed in [1]–[4].

The paper focuses on the design and development of an ANN-based load flow model for power system networks. This model would then provide a load flow solution for the load buses in the IEEE 14-bus system and the Nigerian national 330kV 28-bus system grid.

II. CONVENTIONAL METHODS FOR LOAD FLOW ANALYSIS

Conventional LFA techniques can be categorized into AC load flow methods and DC load flow methods. AC load flow methods deal with calculating bus voltages magnitudes, phase angles, real power, and reactive power flow. It utilizes iterative techniques such as the Gauss-Siedel method, Newton-Raphson method, and Fast decoupled approach. In contrast, the DC load flow methods are used for contingency analysis [5].

A. Gauss-Siedel Load Flow Analysis

The Gauss-Siedel load flow analysis method utilizes the Gauss-Siedel iterative method; in this method, an initial guess of the unknown quantities is required. The actual values of these quantities are calculated and then updated at the end of each iteration. The process continues until convergence is met. Equation (1) gives the formula for this method.

$$V_i = \frac{1}{Y_{ii}} \left(\frac{P_i - jQ_i}{v_i^*} - \sum_{\substack{k=1 \\ k \neq i}}^n Y_{ik} V_k \right) \quad (1)$$

This method has one main disadvantage making it unsuitable for large power systems as convergence time increases with system size. Other disadvantages are listed in [6].

B. Newton-Raphson Load Flow Analysis

This method is the most efficient iterative method currently in use for LFA. In this method, a Jacobian matrix is formed with bus voltages and line admittances expressed in polar form. The method requires an initial guess of the unknown quantities; however, the chosen value must be near the expected solution to convergence quickly. Equations (2) and (3) describes the method.

$$P_i = \sum_{k=1}^n (V_i V_k Y_{ik}) \cos(\delta_i - \delta_k - \theta_{ik}) \quad (2)$$

$$Q_i = \sum (V_i V_k Y_{ik}) \sin(\delta_i - \delta_k - \theta_{ik}) \quad (3)$$

The Newton-Raphson method is widely accepted and used because convergence is guaranteed even in large networks. Another reason for its popularity is highlighted in [6].

C. Fast Decoupled Load Flow Analysis

The method is an extension of the Newton-Raphson load flow method in polar coordinate; it employs the sparse matrix technique, which requires less computer storage and running time. The mathematical formula for this method is given in equation (4) and (5).

$$\Delta P = J_1 \Delta \delta = \left(\frac{\partial P}{\partial \delta} \right) \Delta \delta \tag{4}$$

$$\Delta Q = J_4 |\Delta V| = \left(\frac{\partial Q}{\partial |V|} \right) |\Delta V| \tag{5}$$

For this study, the Newton-Raphson method (N-R) is used because of the numerous advantages of the technique highlighted in [6].

III. NON-CONVENTIONAL METHODS FOR LOAD FLOW ANALYSIS

A. Fuzzy Logic

Fuzzy logic deals with imprecise values that lie between 0 and 1; that is, the logic recognizes more than only true or false values, making it a potent tool for solving non-linear algebraic equations.

The authors in [1] approached the load flow problem using two intelligent techniques (artificial neural network and fuzzy logic). The paper presented load flow analysis using an adaptive neuro-fuzzy inference system (ANFIS); the proposed technique showed clear improvements over conventional speed and feasibility techniques.

In [3], the authors proposed a fuzzy logic-based load flow analysis method. The proposed approach utilizes the triangular and Gaussian membership functions and has its foundation on the fast decoupled load flow method. This efficacy of the proposed approach was tested on the IEEE 9 bus system. The authors found that the proposed approach was faster than the Newton-Raphson method.

In [6], the authors proposed a fuzzy logic-based load flow analysis technique that computes the voltage magnitude and angle of buses in a power system. The authors successfully reduced computation time by using a Gaussian membership function instead of the triangular function.

B. Artificial Neural Networks (ANNs)

In [7], the authors proposed a multilayer feed-forward neural network to determine bus voltages and angles of a radial distribution system for any given load without carrying out conventional load flow analysis. The efficacy of the proposed approach was tested on a sample 33 bus system.

The authors in [8] proposed an ANN-based load flow analysis using the multilayer perceptron neural network trained using the Levenberg-Marquardt algorithm to compute voltage magnitude and angles IEEE 30 bus system. Other non-conventional techniques for load flow analysis can be found in [9].

IV. MATERIALS AND METHODS

This section gives details of the materials and methods used in this study. This section is divided into two subsections: one that provides details of the selected power system networks

while the other sheds light on the data collection process, the selected ANN variant used in this study, and the variant's training.

i. Dataset Material

This paper has two case studies: the IEEE 14-bus system and the Nigerian 330kV 28-bus National Grid (NNG). A brief description of the two networks is given in this section.

a. IEEE 14-Bus System

The IEEE 14-bus system is a standard test bus with five (5) generator buses, nine (9) load buses, and twenty (20) interconnected lines. Bus 1 is selected as the slack bus.

b. NNG 330kV 28-Bus System

The suitability and validity of the proposed approach were confirmed by carrying out tests on the NNG 330kV 28-bus system using the approach. This bus system consists of 9 generator buses, 19 load buses, and 31 interconnected lines, as shown in figure 2. Bus 1, the Egbin power plant, is selected as the slack bus per the authors' findings in [11]. The bus and line data for the NNG 330kV 28-bus system was gotten from the Transmission Company of Nigeria and compiled by the author [12].

ii. METHODOLOGY

a. Data Collection

The data used in this study was generated by running Newton-Raphson load flow analysis in MATLAB. The following parameters were collected real power, reactive power, voltage magnitude, and voltage angle of the load buses used as the ANN input features. This process stops once load flow analysis fails to converge for each of the testbeds.

A total of 1,539 samples were generated for the IEEE 14-bus system and 18,050 samples for the NNG 300Kv 28-bus system. For the two case studies, the data generated were concatenated in an excel spreadsheet to form the study datasets.

b. Artificial Neural Network

Artificial neural networks (ANNs) are biologically inspired computational networks that consist of a set of elementary neurons in highly interconnected layers [13]. These networks are capable of exploring the relationship between several variables with very high precision.

Like the human brain, artificial neural networks can learn from input data with or without an instructor and perform if-then deductive reasoning to solve several non-linear problems through neurons' help; these artificial neurons are modelled after biological neurons shown in figure 1.

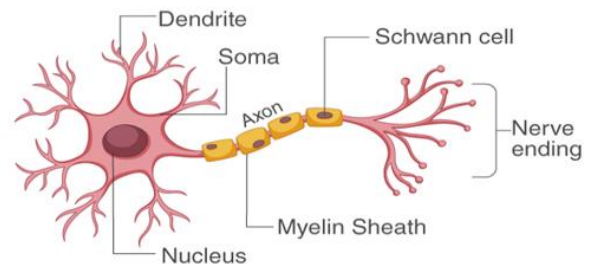


Fig. 1: Structure of a biological neuron

Over the past decade, ANN has become increasingly popular as it is often used to solve non-linear modelling problems [14]. As earlier stated, ANNs are composed of

numerous processing units called neurons, and these neurons consist of a group of interconnected links known as nodes. These nodes are associated with weights w_{kj} ; each weight is multiplied by an input x_j . This process's output is then summed with an external bias b_k used to modify the weighted sum v_k . The output y_k is passed to an activation function ϕ , which reduces its amplitude then determines the state on the neuron (on/off). The neural network process is represented by equations (6) and (7).

$$net_k = \sum_{j=1}^m (w_{kj}) + b_k \tag{6}$$

$$y_k = \phi(v_k)(net_k) \tag{7}$$

Where: w_{kj} is the nodes' weights, x_j is the input, b_k is the bias. v_k is the sum of the weighted output, ϕ is the activation function, and y_k is the neural network's output. Figure 2 shows the model representing a neuron.

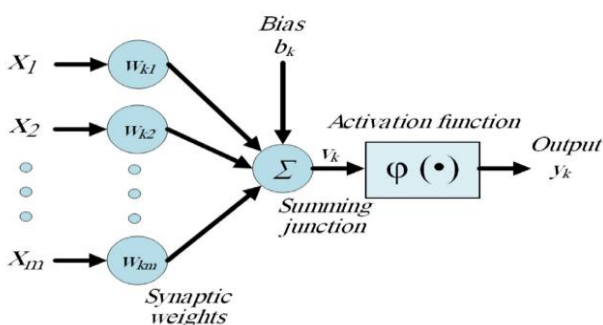


Fig. 2: Model depiction of a neuron

Different activation functions could be used in an ANN model; some of the most commonly used functions are sigmoid, linear, Gaussian, and Gaussian complement functions.

Determination of Structure of the Artificial Neural Network

Two (2) artificial neural network variants were frequently used; were tested to determine which would best suit the generated datasets. The two models are the radial basis function (RBF) network and Multilayer Perceptron Neural Network (MLPNN) [14]; to determine which ANN variant best suit the datasets from the above mentioned, both were trained. During training, the number of hidden layers and neurons in these layers were varied. This approach was adopted because a consensus on determining the number of hidden layers and neurons in those layers have not been reached. However, several techniques and rules of thumb exist to help ease this difficulty [15]. The best model and architecture were chosen based on the Mean Square Error (MSE) performance parameter.

Training of the aforementioned neural network variants was done using a sample of the dataset; the experiment results are presented in Table I.

ANN Variant	MSE
RBF	3.3884×10^{-5}
MLP	2.9142×10^{-5}

Table I shows that the MLPNN in this study outperformed the RBF neural network with an MSE value of 2.9142. For this reason, an MLPNN was selected.

Structure of the Artificial Neural Network

The basic structure of the MLPNN consists of one input layer, one output layer, and one or more hidden layers with interconnected weights and biases, as shown in figure 3. The mathematical equations governing this ANN variant can be found in [16].

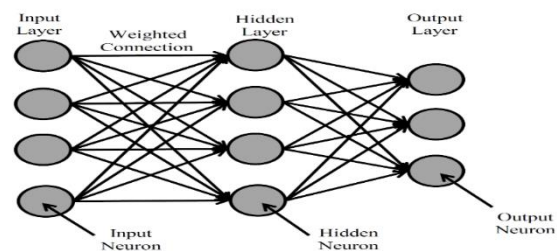


Fig.3: Basic structure of an MLPNN

In this study, two different ANN models based on the multilayer perceptron neural network (MLPNN) were developed in MATLAB. The first model was used for the IEEE 14-bus and the other for the NNG 330kV 28-bus. Figure 4 shows the network diagram for the IEEE 14-bus ANN model. The MLPNN model consists of three layers. The input layer has eighteen (18) neurons, with each representing the input features. These features are the real and reactive powers for the nine (9) load buses in the IEEE 14-bus system.

The hidden layer has thirty (30) neurons chosen based on a trial and error approach. The output layer consists of eighteen (18) neurons representing the study's output variables.

Figure 5 shows the network diagram for the NNG 28-bus ANN model. The input layer has thirty-eight (38) neurons, with each representing the input features. These features are the real and reactive powers for the nineteen (19) load buses in the NNG 28-bus system. The network has two hidden layers with forty (40) and thirty (30) neurons in each layer, and the output layer consists of thirty-eight (38) neurons representing the output variables of the study.

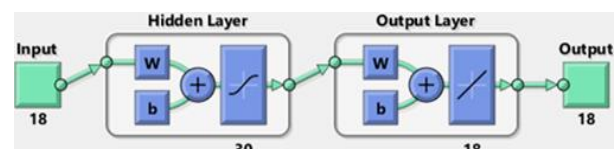


Fig. 4: IEEE 14 load flow network diagram

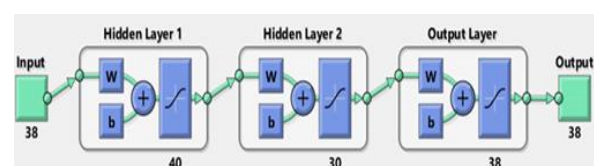


Fig. 5: NNG load flow network diagram

Seventy per cent of the data generated for both case studies were used for training. The remaining thirty per cent of the dataset was further split into validation and test sets, with each set containing 15% of the generated data for both case studies. The two MLPNN models were trained using a back-propagation algorithm. Training is the process by which the neural network's weights are modified to ensure the network produces the desired output or improves the network's output [17].

The activation function used between the input and output layers is the purely linear (purelin) function. The hyperbolic tangent sigmoid (tansig) function is used in the hidden layer of the model. The mathematical expression for these functions is given in equations (8) and (9).

$$f(z) = \text{purelin}(z) = z \tag{8}$$

$$f(z) = \text{tansig}(z) = \frac{2}{(1 + e^{(-2z)}) - 1} \tag{9}$$

A non-linear activation function is used in the developed models' hidden layer due to the non-linear nature of the load flow problem and literature reviewed [13]. However, another reason for using a non-linear activation function in the hidden layer is to ensure the hidden neurons are more sensitive than mere perceptrons [18].

In this study, the Levenberg-Marquardt (LM) algorithm was used in training the network. In [19], the author found that neural networks trained using LM and gradient descent with adaptive learning back-propagation (GDA) gave the best results for load flow analysis. The regression plots for both learning algorithms were approximately equal to 1. Other literature-based reasons which justify the use of LM over GDA is given below:

1. LM assures problem solving through its adaptive behaviour [20].
2. LM combines the Gauss-Newton method's best attributes and the steepest descent method in high speed and stability [21].

The above-stated reasons informed the choice and use of LM over GDA in this study.

Tackling the inherent stability issue faced by artificial neural networks and preventing the models' from over-fitting, the neural networks' results were cross-validated. The models were trained ten times, then the resultant R values for each of the iteration was averaged. This value was then taken as the overall R-value for the models.

c. Performance Evaluation

The Mean Square Error (MSE) was used to assess its performance. The mean square error must be as close to zero (0) as possible because this speaks to the developed neural networks' quality. The performance criterion is described by equation (10).

$$MSE = \frac{\sum_{i=1}^N (d_i - y_i)^2}{N} \tag{10}$$

N is the number of observations, d_i is the target output, and y_i is the predicted output.

V. RESULTS AND DISCUSSION

In this section, the results of the study are given in relevant figures and tables. Related discussions are also made to ensure an adequate understanding of the obtained results.

A. Load Flow Analysis on IEEE 14-bus system

Table II presents voltage magnitude and voltage phase angles obtained by N-R and ANN in per unit for the nine load buses in the IEEE 14-bus system at the base case. The base case refers to the normal operating condition of the system

Table II
Comparison of Load Flow Results by N-R and ANN on the IEEE 14-Bus at Base

Bus no.	Actual Value		ANN Value		Errors	
	Voltage	Angle	Voltage	Angle	Voltage	Angle
4	1.001	11.130	0.999	-1.120	0.002	-0.010
5	1.007	-9.543	1.010	-9.526	-0.003	-0.017
7	0.983	14.576	0.987	-14.578	-0.004	0.002
9	0.965	16.455	0.966	-16.463	-0.001	0.008
10	0.961	16.696	0.963	-16.694	-0.002	-0.002
11	0.972	16.459	0.972	-16.289	0.000	-0.170
12	0.973	16.918	0.973	-16.703	0.000	-0.215
13	0.967	16.981	0.966	-16.981	0.001	0.000
14	0.946	17.877	0.944	-17.884	0.002	0.007

The results presented in Table II show that the developed model could accurately predict both voltage magnitude and voltage phase angle of load buses in the network at the base case.

From the table, bus 14 is the only bus whose voltage falls below the acceptable voltage tolerance margin of $\pm 5\%$ with a magnitude of 0.0946 p.u.; this indicates that the 14th could have some voltage stability issues. It was also validated by [19], [22]. However, further investigation is needed before any bus can be declared the weakest in any power system.

Table III shows the result of load flow analysis on the 4th bus in the IEEE 14-bus system.

Table III
Comparison of Load Flow Results by N-R and ANN on 4th bus at - 7.8MVar

Bus no.	Actual Value		ANN Value		Errors	
	Voltage	Angle	Voltage	Angle	Voltage	Angle
4	1.001	-11.130	0.999	-1.120	0.002	-0.010
5	1.007	-9.543	1.010	-9.526	-0.003	-0.017
7	0.983	-14.576	0.987	-14.578	-0.004	0.002
9	0.965	-16.455	0.966	-16.463	-0.001	0.008
10	0.961	-16.696	0.963	-16.694	-0.002	-0.002
11	0.972	-16.459	0.972	-16.289	0.000	-0.170
12	0.973	-16.918	0.973	-16.703	0.000	-0.215
13	0.967	-16.981	0.966	-16.981	0.001	0.000
14	0.946	-17.877	0.944	-17.884	0.002	0.007

Table IV shows the result of load flow analysis on the 7th bus in the IEEE 14-bus system.

Table IV
Comparison of Load Flow Results by N-R and ANN on 7th bus at 8.7105MVar

Bus no.	Actual Value		ANN Value		Errors	
	Voltage	Angle	Voltage	Angle	Voltage	Angle
4	0.991	-11.122	0.977	-11.144	0.013	0.022
5	0.998	-9.523	0.989	-9.512	0.009	-0.011
7	0.971	14.638	0.960	-14.635	0.010	-0.003
9	0.953	-16.560	0.957	-16.556	-0.004	-0.004
10	0.949	-16.811	0.931	-16.801	0.019	-0.010
11	0.961	-16.578	0.947	-16.392	0.014	-0.186
12	0.963	-17.058	0.966	-16.860	-0.003	-0.199
13	0.957	-17.119	0.950	-17.101	0.007	-0.018
14	0.935	-18.025	0.947	-18.016	-0.013	-0.009

Table V shows the result of load flow analysis on the 12th bus in the IEEE 14-bus system.

Table V
Comparison of Load Flow Results by N-R and ANN on 12th bus at 5.668MVar

Bus no.	Actual Value		ANN Value		Errors	
	Voltage	Angle	Voltage	Angle	Voltage	Angle
4	0.992	-11.146	0.988	-11.108	0.004	-0.039
5	0.999	-9.532	0.994	-9.494	0.005	-0.038
7	0.978	-14.663	0.975	-14.666	0.003	0.002
9	0.958	-16.580	0.960	-16.574	-0.002	-0.006
10	0.953	-16.819	0.941	-16.830	0.013	0.011
11	0.963	-16.561	0.955	-16.428	0.008	-0.133
12	0.957	-16.788	0.953	-16.618	0.005	-0.169
13	0.955	-17.048	0.941	-17.043	0.014	-0.005
14	0.937	-18.000	0.939	-18.003	-0.002	0.003

Figure 6 shows that the developed neural network can accurately carry out load flow analysis as the predicted values for voltage magnitudes of load buses in the system obtained from the Newton-Raphson approach used for verifying the artificial neural network system.

Figure 7 gives the graphical representation of the relationship between the actual and predicted voltage magnitude values and the angle at a reactive power loading of -7.8MVar for bus 4 in the IEEE 14-bus system.

Figure 8 shows that the developed neural network can accurately carry out load flow analysis. The predicted values for both voltages angles closely match the values obtained from the Newton-Raphson approach used for verifying the artificial neural network system.

The developed neural network model had a regression value of 0.9884 after cross-validation was done and an MSE of 1.6701×10^{-3} , as given in figure 10.

In [19], the authors implemented an MLPNN to carry out load flow studies on the IEEE-14 bus system using LM as the training algorithm. An R-value of 0.97976 was obtained. However, the proposed model's R-value surpasses.

B. NNG 330kV 28-bus system

Table VI presents voltage magnitudes and voltage phase angles obtained by N-R and ANN per unit for the nineteen load buses in the NNG 28-bus system at the base case.

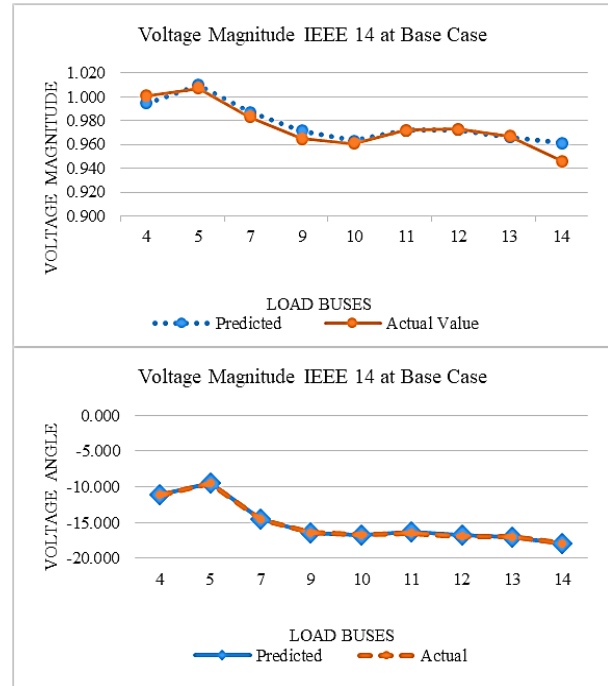


Fig. 6: IEEE - N-R vs ANN Load Flow Results at Base Case

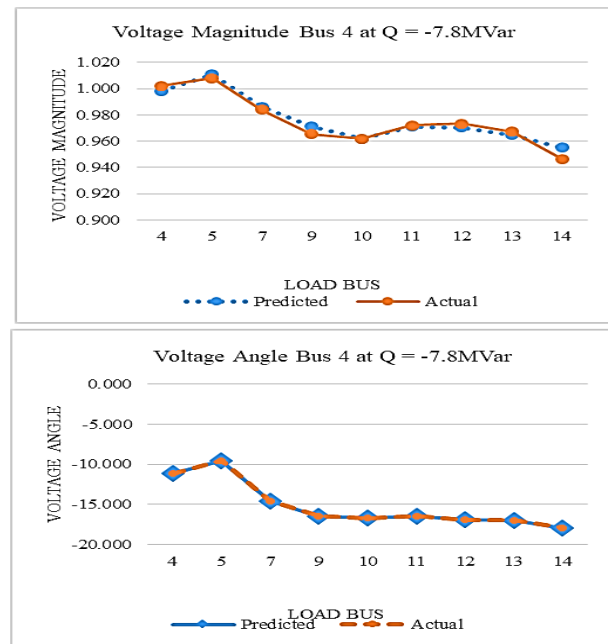


Fig. 7: IEEE - N-R vs ANN Load Flow Results at Q = -7.8MVar

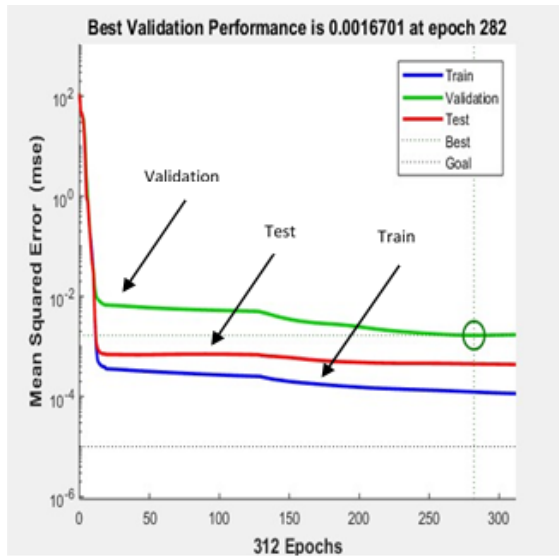


Fig. 8: Performance plot for ANN-based load flow

C. NNG 330kV 28-bus system

Table VI presents voltage magnitudes and voltage phase angles obtained by N-R and ANN per unit for the nineteen load buses in the NNG 28-bus system at the base case.

Table VI
Comparison of Load Flow Results by N-R and ANN on NNG 28-Bus at Base case

Bus no.	Actual Value		ANN Value		Errors	
	Voltage	Angle	Voltage	Angle	Voltage	Angle
3	1.040	-0.570	0.958	-0.552	0.082	-0.018
4	0.969	-6.097	1.003	-6.125	-0.034	0.028
5	0.985	-5.170	0.988	-5.135	-0.003	-0.035
6	1.027	-15.795	1.007	-15.740	0.020	-0.055
7	1.046	-15.699	0.999	-15.748	0.047	0.048
8	1.011	-15.229	1.030	-15.211	-0.019	-0.017
9	0.936	-7.921	0.946	-7.922	-0.011	0.001
10	0.969	-4.808	0.948	-4.812	0.021	0.004
12	1.008	-10.077	1.023	-10.025	-0.015	-0.052
13	0.905	-20.087	0.915	-20.200	-0.010	0.113
14	0.949	-17.139	0.920	-16.964	0.028	-0.176
15	1.010	11.578	0.974	11.459	0.036	0.119
16	0.923	-13.753	0.926	-13.775	-0.003	0.022
17	1.046	10.801	1.030	10.754	0.016	0.046
19	0.961	-6.356	0.987	-6.334	-0.026	-0.023
20	0.963	-8.438	0.947	-9.139	0.016	0.701
22	0.833	-18.485	0.921	-18.430	-0.087	-0.055
25	0.964	0.873	0.968	1.049	-0.004	-0.176
26	1.000	-7.243	0.960	-7.045	0.040	-0.198

From the result presented in Table VI, the ANN model results are also promising. The developed neural network could accurately predict both voltage magnitude and voltage phase angle of load buses in the base case network. The table shows that several buses (9, 13, 14, 16, 19, and 22) violate the $\pm 5\%$ voltage tolerance margin set by the Nigerian Electricity

Regulation Commission (NERC). The results obtained are validated by [12].

Table VII
Comparison of Load Flow Results by N-R and ANN on 3rd bus at 282.182MVar

Bus no.	Actual Value		ANN Value		Errors	
	Voltage	Angle	Voltage	Angle	Voltage	Angle
3	1.037	-0.547	0.960	-0.523	0.077	-0.025
4	0.969	-6.097	1.002	-6.122	-0.032	0.026
5	0.985	-5.170	0.988	-5.145	-0.002	-0.025
6	1.027	-15.795	1.008	-15.758	0.019	-0.037
7	1.046	-15.699	1.019	-15.829	0.028	0.130
8	1.011	-15.229	1.028	-15.225	-0.017	-0.004
9	0.936	-7.921	0.948	-8.273	-0.012	0.353
10	0.969	-4.808	0.950	-4.808	0.019	-0.001
12	1.008	-10.077	1.022	-10.034	-0.014	-0.043
13	0.905	-20.087	0.911	-20.186	-0.007	0.100
14	0.949	-17.139	0.917	-17.026	0.031	-0.114
15	1.010	11.578	0.972	11.527	0.037	0.050
16	0.923	-13.753	0.926	-13.771	-0.003	0.018
17	1.046	10.801	1.048	10.878	-0.001	-0.077
19	0.961	-6.356	0.985	-6.319	-0.024	-0.037
20	0.963	-8.438	0.956	-8.455	0.007	0.017
22	0.833	-18.485	0.920	-18.436	-0.087	-0.049
25	0.964	0.873	0.967	0.974	-0.003	-0.102
26	1.000	-7.243	0.960	-7.094	0.041	-0.149

Table VIII
Comparison of Load Flow Results by N-R and ANN on 5th bus at 514.180MVar

Bus no.	Actual Value		ANN Value		Errors	
	Voltage	Angle	Voltage	Angle	Voltage	Angle
3	1.040	-0.570	0.963	-0.674	0.077	0.104
4	0.967	-6.103	0.983	-6.093	-0.017	-0.011
5	0.983	-5.172	0.916	-5.140	0.067	-0.032
6	1.026	-15.842	1.007	-15.844	0.020	0.003
7	1.046	-15.749	0.993	-15.702	0.053	-0.046
8	1.011	-15.275	1.000	-15.246	0.010	-0.029
9	0.934	-7.944	0.933	-8.011	0.001	0.068
10	0.968	-4.827	0.945	-4.923	0.023	0.096
12	1.008	-10.117	0.992	-10.164	0.016	0.047
13	0.904	-20.133	0.874	-20.218	0.030	0.085
14	0.948	-17.184	0.890	-17.024	0.058	-0.160
15	1.010	11.567	1.004	11.378	0.006	0.189
16	0.923	-13.782	0.912	-13.662	0.011	-0.119
17	1.046	10.790	1.042	10.847	0.005	-0.057
19	0.961	-6.385	1.004	-6.497	-0.043	0.112
20	0.963	-8.460	0.930	-9.193	0.033	0.733
22	0.833	-18.507	0.894	-18.381	-0.061	-0.127
25	0.964	0.839	0.987	0.762	-0.023	0.077
26	1.000	-7.262	0.935	-7.171	0.065	-0.091

Table VII shows the result of load flow analysis on the 3rd bus in the NNG 28-bus system.

Table VIII shows the result of load flow analysis on the 5th bus in the NNG 28-bus system

Table IX shows the result of load flow analysis on the 16th bus in the NNG 28-bus system.

Table IX
Comparison of Load Flow Results by N-R and ANN on 16th bus at 65.735MVar

Bus no.	Actual Value		ANN Value		Errors	
	Voltage	Angle	Voltage	Angle	Voltage	Angle
3	1.037	-0.547	0.960	-0.523	0.077	-0.025
4	0.969	-6.097	1.002	-6.122	-0.032	0.026
5	0.985	-5.170	0.988	-5.145	-0.002	-0.025
6	1.027	-15.795	1.008	-15.758	0.019	-0.037
7	1.046	-15.699	1.019	-15.829	0.028	0.130
8	1.011	-15.229	1.028	-15.225	-0.017	-0.004
9	0.936	-7.921	0.948	-8.273	-0.012	0.353
10	0.969	-4.808	0.950	-4.808	0.019	-0.001
12	1.008	-10.077	1.022	-10.034	-0.014	-0.043
13	0.905	-20.087	0.911	-20.186	-0.007	0.100
14	0.949	-17.139	0.917	-17.026	0.031	-0.114
15	1.010	11.578	0.972	11.527	0.037	0.050
16	0.923	-13.753	0.926	-13.771	-0.003	0.018
17	1.046	10.801	1.048	10.878	-0.001	-0.077
19	0.961	-6.356	0.985	-6.319	-0.024	-0.037
20	0.963	-8.438	0.956	-8.455	0.007	0.017
22	0.833	-18.485	0.920	-18.436	-0.087	-0.049
25	0.964	0.873	0.967	0.974	-0.003	-0.102
26	1.000	-7.243	0.960	-7.094	0.041	-0.149

From tables VII-IX, the negligible error between the actual and predicted values of the voltage magnitude and voltage phase angles for the specific bus in the NNG 28-bus system could be seen to show the efficacy of the proposed approach further.

Figure 9 shows the negligible error between the predicted and actual values for the base case. From the figures, it can be noticed that the values obtained by N-R and ANN are very close to each other, and the error between them is minimal.

The figure reveals that the developed neural network could accurately carry out load flow analysis as the predicted values for voltage magnitudes of load buses in the system closely match the values obtained from the Newton-Raphson approach used to verify the artificial neural network system.

Figure 10 shows the graphical representation of the relationship between the actual and predicted voltage magnitude values and angle at a reactive power loading of 282.182MVar for bus 3.

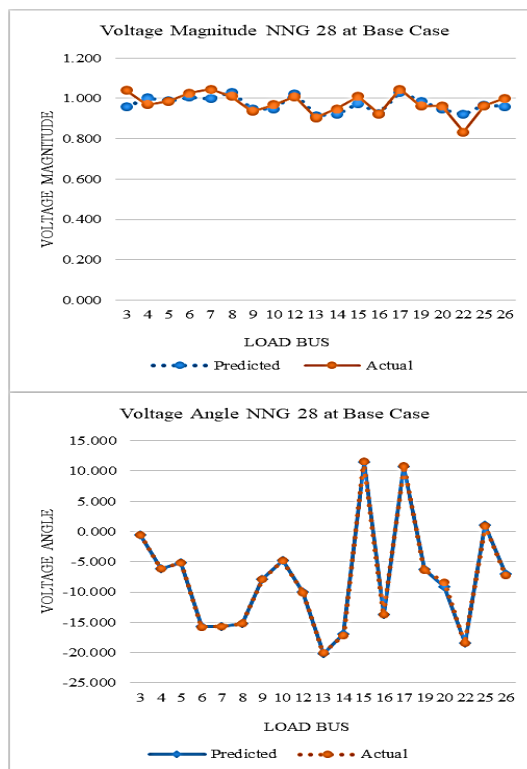


Fig. 9: NNG - N-R vs ANN Load Flow Results at Base Case

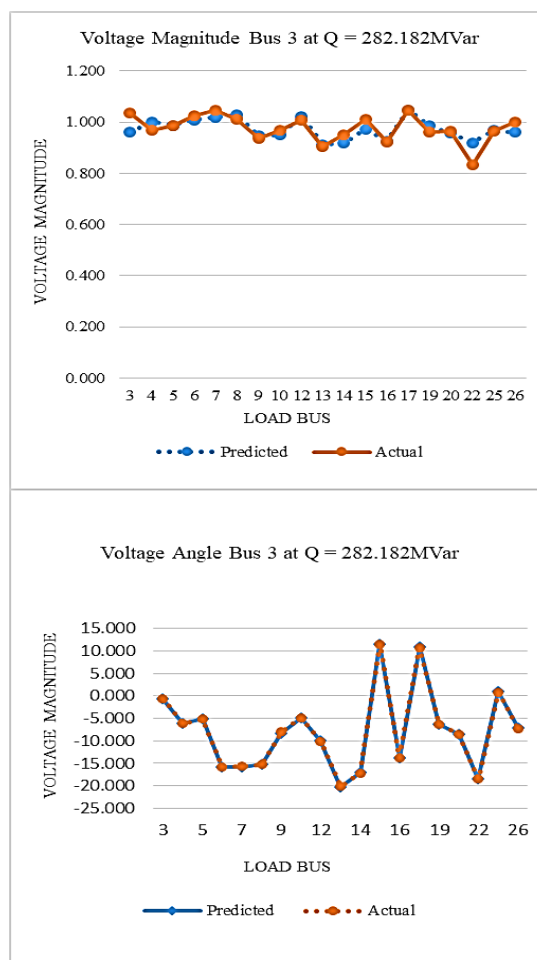


Fig. 10: NNG - N-R vs ANN Load Flow Results at Q = 282.182MVar

All the figures presented that the developed neural network can accurately carry out load flow analysis as the predicted

values for voltage magnitude and angles closely match the values obtained from the dataset used for verifying the artificial neural network system.

The developed neural network model had a regression value of 0.99972 with an MSE of 3.8624×10^{-3} as given in figures 11.

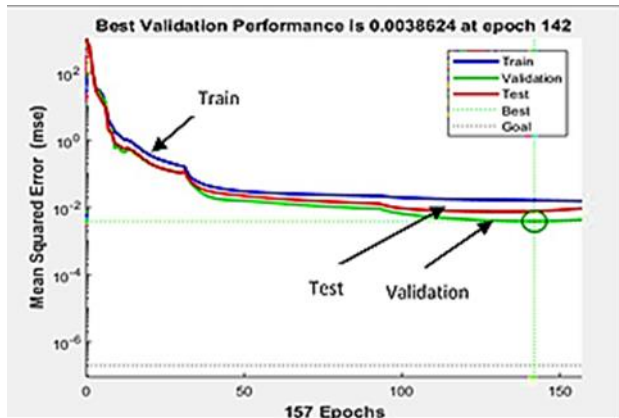


Fig. 11: Performance plot for ANN-based load flow

VI. Conclusion

Load flow analysis/studies are central to power system planning and operation. Advancements in technology have led to the development of several techniques for solving the load flow problem. In this paper, some techniques for carrying out this study are discussed. Although these conventional methods are highly capable of providing a solution to the load flow problem, they have drawbacks that have made researchers seek out faster ways to carry out load flow analysis.

The proposed approach has proved that non-conventional methods can be used to carry out load flow analysis; the results obtained from this study also aligns with the findings of other authors who had used conventional methods. After comparing the two methods' results, the observed error between the conventional and non-conventional ANN method was negligible, thus validating the proposed approach.

ACKNOWLEDGEMENTS

The authors would like to acknowledge and appreciate the Covenant University Centre for Research, Innovation, and Discovery to publish this research work.

REFERENCES

- [1] D. Abdellah and L. Djamel, "Power flow analysis using adaptive neuro-fuzzy inference systems," *2015 3rd International Renewable and Sustainable Energy Conference (IRSEC)*, 2015, pp. 1–5, doi: 10.1109/IRSEC.2015.7455102.
- [2] P. T. Son and N. Voropai, "The Major Outage in South Vietnam in 2013 : The Nature of Blackout, Security Measures and Strategy of National Power System Modernization," in *International Conference on Problem of Critical Structures*, 2015, pp. 177–182.
- [3] U. Buragohain and T. Boruah, "Fuzzy logic based load flow analysis," in *2017 International Conference on Algorithms, Methodology, Models and Applications in Emerging Technologies (ICAMMAET)*, 2017, pp. 1–6, doi: 10.1109/ICAMMAET.2017.8186736.
- [4] T. M. Mohan and T. Nireekshana, "A Genetic Algorithm for Solving Optimal Power Flow Problem," in *2019 3rd International Conference on Electronics, Communication and Aerospace Technology (ICECA)*, 2019, pp. 1438–1440, doi: 10.1109/ICECA.2019.8822090.
- [5] P. S. R. Murty, "Load Flow Analysis," in *Electrical Power Systems*, 2017, pp. 527–587.
- [6] S. Dixit, L. Srivastava, and G. Agnihotri, "Power flow analysis using fuzzy logic," in *2006 IEEE Power India Conference*, 2006, p. 7 pp., doi: 10.1109/POWERI.2006.1632605.
- [7] A. Arunagiri, B. Venkatesh, and K. Ramasamy, "Artificial neural network approach-an application to radial load flow algorithm," *IEICE Electron. Express*, vol. 3, no. 14, pp. 353–360, 2006, doi: 10.1587/elex.3.353.
- [8] V. L. Paucar and M. J. Rider, "Artificial neural networks for solving the power flow problem in electric power systems," *Electr. Power Syst. Res.*, vol. 62, no. 2, pp. 139–144, 2002, doi: 10.1016/S0378-7796(02)00030-5.
- [9] B. S. P. Bhowmik P S, Rajan D V, "Load Flow Analysis: An Overview," *Int. J. Electr. Comput. Eng. Electron. Commun. Eng.*, vol. 6, no. 3, pp. 263–268, 2012.
- [10] R. Christie, "Power Systems Test Case Archive," 1996. [Online]. Available: http://labs.ece.uw.edu/pstca/pf14/pg_tca14bus.htm. [Accessed: 19-Dec-2020].
- [11] I. A. Samuel, O. N. Marian, and A. Abudulkareem, "Investigating The Selection Of A Suitable Slack Bus: A Case Study Of The Multi-Generating Stations Of The Nigerian 330-kV Power System Network," *Int. J. Electr. Electron. Eng. Stud.*, vol. 2, no. 1, pp. 1–12, 2014.
- [12] I. A. Samuel, "A New Voltage Stability Index For Predicting Voltage Collapse In Electrical Power System Networks," Covenant University, 2017.
- [13] R. Shetty, "Power System Voltage Stability Analysis and Assessment Using Artificial Neural Network," California State University, 2014.
- [14] A. H. Elsheikh, S. W. Sharshir, M. Abd Elaziz, A. E. Kabeel, W. Guilan, and Z. Haiou, "Modeling of solar energy systems using artificial neural network: A comprehensive review," *Sol. Energy*, vol. 180, no. January, pp. 622–639, 2019, doi: 10.1016/j.solener.2019.01.037.
- [15] K. G. Sheela and S. N. Deepa, "Review on Methods to Fix Number of Hidden Neurons in Neural Networks," *Math. Probl. Eng.*, vol. 2013, no. 10, pp. 1–11, 2013, doi: 10.1155/2013/425740.
- [16] A. Abudulkareem, A. Adesanya, O. Popoola, and C. O. A. Awosope, "Predicting insulation thickness in thermoplastic extrusion process in Nigeria cable industries using artificial neural network," *Eng. Lett.*, vol. 27, no. 4, pp. 907–917, 2019.
- [17] Q. K. Al-Shayea, "Neural networks to predict stock market price," *Lect. Notes Eng. Comput. Sci.*, vol. 1, pp. 371–377, 2017.
- [18] J. J. Popoola and R. Van Olst, "The performance evaluation of a spectrum sensing implementation using an automatic modulation classification detection method with a Universal Software Radio Peripheral," *Expert Syst. Appl.*, vol. 40, no. 6, pp. 2165–2173, 2013, doi: 10.1016/j.eswa.2012.10.047.
- [19] S. Tiwari, M. A. Ansari, K. Kumar, S. Chaturvedi, M. Singh, and S. Kumar, "Load Flow Analysis of IEEE 14 Bus System Using ANN Technique," in *2018 International Conference on Sustainable Energy, Electronics, and Computing Systems (SEEMS)*, 2018, no. 1, pp. 1–5, doi: 10.1109/SEEMS.2018.8687353.
- [20] Y.-C. Du and A. Stephanus, "Levenberg-Marquardt Neural Network Algorithm for Degree of Arteriovenous Fistula Stenosis Classification Using a Dual Optical Photoplethysmography Sensor," *Sensors*, vol. 18, no. 7, p. 2322, Jul. 2018, doi: 10.3390/s18072322.
- [21] P. Wilson and H. A. Mantooth, "Model-Based Optimization Techniques," in *Model-Based Engineering for Complex Electronic Systems*, Elsevier, 2013, pp. 347–367.
- [22] I. A. Samuel, J. Katende, C. O. A. Awosope, and A. A. Awelewa, "Prediction of Voltage Collapse in Electrical Power System Networks using a New Voltage Stability Index," *Int. J. Appl. Eng. Res.*, vol. 12, pp. 190–199, 2017.